Measurement of the Cross Section for $e^+e^- \to$ Hadrons at Energies from 2.2324 to 3.6710 GeV

M. Ablikim,[1] M. N. Achasov,[10,b] P. Adlarson,[66] S. Ahmed,[14] M. Albrecht,[4] R. Aliberti,[27] A. Amoroso,[65a,65c] M. R. An,[31] Q. An,[62,48] X. H. Bai,[56] Y. Bai,[47] O. Bakina,[28] R. Baldini Ferroli,[22a] I. Balossino,[23a] Y. Ban,[37,h] K. Begzsuren,[25] N. Berger,[27] M. Bertani,[22a] D. Bettoni,[23a] F. Bianchi,[65a,65c] J. Bloms,[59] A. Bortone,[65a,65c] I. Boyko,[28] R. A. Briere,[5] H. Cai,[67] X. Cai,[1,48] A. Calcaterra,[22a] G. F. Cao,[1,53] N. Cao,[1,53] S. A. Cetin,[52a] J. F. Chang,[1,48] W. L. Chang,[1,53] G. Chelkov,[28,a] D. Y. Chen,[6] G. Chen,[1] H. S. Chen,[1,53] M. L. Chen,[1,48] S. J. Chen,[34] X. R. Chen,[24] Y. B. Chen,[1,48] Z. J. Chen,[19,i] W. S. Cheng,[65c] G. Cibinetto,[23a] F. Cossio,[65c] X. F. Cui,[35] H. L. Dai,[1,48] X. C. Dai,[1,53] A. Dbeyssi,[14] R. E. de Boer,[4] D. Dedovich,[28] Z. Y. Deng,[1] A. Denig,[27] I. Denysenko,[28] M. Destefanis,[65a,65c] F. De Mori,[65a,65c] Y. Ding,[32] C. Dong,[35] J. Dong,[1,48] L. Y. Dong,[1,53] M. Y. Dong,[1,48,53] X. Dong,[67] S. X. Du,[70] Y. L. Fan,[67] J. Fang,[1,48] S. S. Fang,[1,53] Y. Fang,[1] R. Farinelli,[23a] L. Fava,[65b,65c] F. Feldbauer,[4] G. Felici,[22a] C. Q. Feng,[62,48] J. H. Feng,[49] M. Fritsch,[4] C. D. Fu,[1] Y. Gao,[62,48] Y. Gao,[37,h] Y. G. Gao,[6] I. Garzia,[23a,23b] P. T. Ge,[67] C. Geng,[49] E. M. Gersabeck,[57] A. Gilman,[60] K. Goetzen,[11] L. Gong,[32] W. X. Gong,[1,48] W. Gradl,[27] M. Greco,[65a,65c] L. M. Gu,[34] M. H. Gu,[1,48] C. Y. Guan,[1,53] A. Q. Guo,[21] L. B. Guo,[33] R. P. Guo,[39] Y. P. Guo,[9,f] A. Guskov,[28,a] T. T. Han,[40] W. Y. Han,[31] X. Q. Hao,[15] F. A. Harris,[55] K. L. He,[1,53] F. H. Heinsius,[4] C. H. Heinz,[27] Y. K. Heng,[1,48,53] C. Herold,[50] M. Himmelreich,[11,d] T. Holtmann,[4] G. Y. Hou,[1,53] Y. R. Hou,[53] Z. L. Hou,[1] H. M. Hu,[1,53] J. F. Hu,[46,j] T. Hu,[1,48,53] Y. Hu,[1] G. S. Huang,[62,48] L. Q. Huang,[63] X. T. Huang,[40] Y. P. Huang,[1] Z. Huang,[37,h] T. Hussain,[64] N. Hüsken,[21,27] W. Ikegami Andersson,[66] W. Imoehl,[21] M. Irshad,[62,48] S. Jaeger,[4] S. Janchiv,[25] Q. Ji,[1] Q. P. Ji,[15] X. B. Ji,[1,53] X. L. Ji,[1,48] Y. Y. Ji,[40] H. B. Jiang,[40] X. S. Jiang,[1,48,53] J. B. Jiao,[40] Z. Jiao,[17] S. Jin,[34] Y. Jin,[56] M. Q. Jing,[1,53] T. Johansson,[66] N. Kalantar-Nayestanaki,[54] X. S. Kang,[32] R. Kappert,[54] M. Kavatsyuk,[54] B. C. Ke,[42,1] I. K. Keshk,[4] A. Khoukaz,[59] P. Kiese,[27] R. Kiuchi,[1] R. Kliemt,[11] L. Koch,[29] O. B. Kolcu,[52a,m] B. Kopf,[4] M. Kuemmel,[4] M. Kuessner,[4] A. Kupsc,[66] M. G. Kurth,[1,53] W. Kühn,[29] J. J. Lane,[57] J. S. Lange,[29] P. Larin,[14] A. Lavania,[20] L. Lavezzi,[65a,65c] Z. H. Lei,[62,48] H. Leithoff,[27] M. Lellmann,[27] T. Lenz,[27] C. Li,[38] C. H. Li,[31] Cheng Li,[62,48] D. M. Li,[70] F. Li,[1,48] G. Li,[1] H. Li,[62,48] H. Li,[42] H. B. Li,[1,53] H. J. Li,[15] H. N. Li,[46,j] J. L. Li,[40] J. Q. Li,[4] J. S. Li,[49] Ke Li,[1] L. K. Li,[1] Lei Li,[3] P. R. Li,[30,k,l] S. Y. Li,[51] W. D. Li,[1,53] W. G. Li,[1] X. H. Li,[62,48] X. L. Li,[40] Xiaoyu Li,[1,53] Z. Y. Li,[49] H. Liang,[62,48] H. Liang,[1,53] H. Liang,[26] Y. F. Liang,[44] Y. T. Liang,[24] G. R. Liao,[12] L. Z. Liao,[1,53] J. Libby,[20] C. X. Lin,[49] T. Lin,[1] B. J. Liu,[1] C. X. Liu,[1] D. Liu,[14,62] F. H. Liu,[43] Fang Liu,[1] Feng Liu,[6] G. M. Liu,[46,j] H. M. Liu,[1,53] Huanhuan Liu,[1] Huihui Liu,[16] J. B. Liu,[62,48] J. L. Liu,[63] J. Y. Liu,[1,53] K. Liu,[1] K. Y. Liu,[32] L. Liu,[62,48] M. H. Liu,[9,f] P. L. Liu,[1] Q. Liu,[67] Q. Liu,[53] S. B. Liu,[62,48] T. Liu,[1,53] W. M. Liu,[62,48] X. Liu,[30,k,l] Y. Liu,[30,k,l] Y. B. Liu,[35] Z. A. Liu,[1,48,53] Z. Q. Liu,[40] X. C. Lou,[1,48,53] F. X. Lu,[49] H. J. Lu,[17] J. D. Lu,[1,53] J. G. Lu,[1,48] X. L. Lu,[1] Y. Lu,[1] Y. P. Lu,[1,48] C. L. Luo,[33] M. X. Luo,[69] P. W. Luo,[49] T. Luo,[9,f] X. L. Luo,[1,48] X. R. Lyu,[53] F. C. Ma,[32] H. L. Ma,[1] L. L. Ma,[40] M. M. Ma,[1,53] Q. M. Ma,[1] R. Q. Ma,[1,53] R. T. Ma,[53] X. X. Ma,[1,53] X. Y. Ma,[1,48] F. E. Maas,[14] M. Maggiora,[65a,65c] S. Maldaner,[4] S. Malde,[60] Q. A. Malik,[64] A. Mangoni,[22b] Y. J. Mao,[37,h] Z. P. Mao,[1] S. Marcello,[65a,65c] Z. X. Meng,[56] J. G. Messchendorp,[54] G. Mezzadri,[23a] T. J. Min,[34] R. E. Mitchell,[21] X. H. Mo,[1,48,53] N. Yu. Muchnoi,[10,b] H. Muramatsu,[58] S. Nakhoul,[11,d] Y. Nefedov,[28] F. Nerling,[11,d] I. B. Nikolaev,[10,b] Z. Ning,[1,48] S. Nisar,[8,g] Q. Ouyang,[1,48,53] S. Pacetti,[22b,22c] X. Pan,[9,f] Y. Pan,[57] A. Pathak,[1] A. Pathak,[26] P. Patteri,[22a] M. Pelizaeus,[4] H. P. Peng,[62,48] K. Peters,[11,d] J. Pettersson,[66] J. L. Ping,[33] R. G. Ping,[1,53] S. Pogodin,[28] R. Poling,[58] V. Prasad,[62,48] H. Qi,[62,48] H. R. Qi,[51] M. Qi,[34] T. Y. Qi,[9] S. Qian,[1,48] W. B. Qian,[53] Z. Qian,[49] C. F. Qiao,[53] J. J. Qin,[63] L. Q. Qin,[12] X. P. Qin,[9] X. S. Qin,[40] Z. H. Qin,[1,48] J. F. Qiu,[1] S. Q. Qu,[35] K. H. Rashid,[64] K. Ravindran,[20] C. F. Redmer,[27] A. Rivetti,[65c] V. Rodin,[54] M. Rolo,[65c] G. Rong,[1,53] Ch. Rosner,[14] M. Rump,[59] H. S. Sang,[62] A. Sarantsev,[28,c] Y. Schelhaas,[27] C. Schnier,[4] K. Schoenning,[66] M. Scodeggio,[23a,23b] W. Shan,[18] X. Y. Shan,[62,48] J. F. Shangguan,[45] M. Shao,[62,48] C. P. Shen,[9] H. F. Shen,[1,53] X. Y. Shen,[1,53] H. C. Shi,[62,48] R. S. Shi,[1,53] X. Shi,[1,48] X. D. Shi,[62,48] J. J. Song,[40] J. J. Song,[15] W. M. Song,[26,1] Y. X. Song,[37,h] S. Sosio,[65a,65c] S. Spataro,[65a,65c] K. X. Su,[67] P. P. Su,[45] F. F. Sui,[40] G. X. Sun,[1] H. K. Sun,[1] J. F. Sun,[15] L. Sun,[67] S. S. Sun,[1,53] T. Sun,[1,53] W. Y. Sun,[26] X. Sun,[19,i] Y. J. Sun,[62,48] Y. Z. Sun,[1] Z. T. Sun,[1] Y. H. Tan,[67] Y. X. Tan,[62,48] C. J. Tang,[44] G. Y. Tang,[1] J. Tang,[49] J. X. Teng,[62,48] V. Thoren,[66] W. H. Tian,[42] Y. T. Tian,[24] I. Uman,[52b] B. Wang,[1] C. W. Wang,[34] D. Y. Wang,[37,h] H. J. Wang,[30,k,l] H. P. Wang,[1,53] K. Wang,[1,48] L. L. Wang,[1] M. Wang,[40] M. Z. Wang,[37,h] Meng Wang,[1,53] S. Wang,[9,f] W. Wang,[49] W. H. Wang,[67] W. P. Wang,[62,48] X. Wang,[37,h] X. F. Wang,[30,k,l] X. L. Wang,[9,f] Y. Wang,[49] Y. D. Wang,[36] Y. F. Wang,[1,48,53] Y. Q. Wang,[1] Y. Y. Wang,[30,k,l] Z. Wang,[1,48] Z. Y. Wang,[1] Ziyi Wang,[53] Zongyuan Wang,[1,53] D. H. Wei,[12] F. Weidner,[59] S. P. Wen,[1] D. J. White,[57] U. Wiedner,[4] G. Wilkinson,[60] M. Wolke,[66] L. Wollenberg,[4] J. F. Wu,[1,53] L. H. Wu,[1] L. J. Wu,[1,53] X. Wu,[9,f] X. H. Wu,[26] Z. Wu,[1,48] L. Xia,[62,48] H. Xiao,[9,f] S. Y. Xiao,[1]

Z. J. Xiao,[33] X. H. Xie,[37,h] Y. G. Xie,[1,48] Y. H. Xie,[6] T. Y. Xing,[1,53] G. F. Xu,[1] Q. J. Xu,[13] W. Xu,[1,53] X. P. Xu,[45] Y. C. Xu,[53] F. Yan,[9,f] L. Yan,[9,f] W. B. Yan,[62,48] W. C. Yan,[70] H. J. Yang,[41,e] H. X. Yang,[1] L. Yang,[42] S. L. Yang,[53] Y. X. Yang,[12] Yifan Yang,[1,53] Zhi Yang,[24] M. Ye,[1,48] M. H. Ye,[7] J. H. Yin,[1] Z. Y. You,[49] B. X. Yu,[1,48,53] C. X. Yu,[35] G. Yu,[1,53] J. S. Yu,[19,i] T. Yu,[63] C. Z. Yuan,[1,53] L. Yuan,[2] X. Q. Yuan,[37,h] Y. Yuan,[1] Z. Y. Yuan,[49] C. X. Yue,[31] A. A. Zafar,[64] X. Zeng Zeng,[6] Y. Zeng,[19,i] A. Q. Zhang,[1] B. X. Zhang,[1] Guangyi Zhang,[15] H. Zhang,[62] H. H. Zhang,[49] H. H. Zhang,[26] H. Y. Zhang,[1,48] J. J. Zhang,[42] J. L. Zhang,[68] J. Q. Zhang,[33] J. W. Zhang,[1,48,53] J. Y. Zhang,[1] J. Z. Zhang,[1,53] Jianyu Zhang,[1,53] Jiawei Zhang,[1,53] L. M. Zhang,[51] L. Q. Zhang,[49] Lei Zhang,[34] S. Zhang,[49] S. F. Zhang,[34] Shulei Zhang,[19,i] X. D. Zhang,[36] X. Y. Zhang,[40] Y. Zhang,[60] Y. T. Zhang,[70] Y. H. Zhang,[1,48] Yan Zhang,[62,48] Yao Zhang,[1] Z. Y. Zhang,[67] G. Zhao,[1] J. Zhao,[31] J. Y. Zhao,[1,53] J. Z. Zhao,[1,48] Lei Zhao,[62,48] Ling Zhao,[1] M. G. Zhao,[35] Q. Zhao,[1] S. J. Zhao,[70] Y. B. Zhao,[1,48] Y. X. Zhao,[24] Z. G. Zhao,[62,48] A. Zhemchugov,[28,a] B. Zheng,[63] J. P. Zheng,[1,48] Y. H. Zheng,[53] B. Zhong,[33] C. Zhong,[63] L. P. Zhou,[1,53] Q. Zhou,[1,53] X. Zhou,[67] X. K. Zhou,[53] X. R. Zhou,[62,48] X. Y. Zhou,[31] A. N. Zhu,[1,53] J. Zhu,[35] K. Zhu,[1] K. J. Zhu,[1,48,53] S. H. Zhu,[61] T. J. Zhu,[68] W. J. Zhu,[9,f] W. J. Zhu,[35] Y. C. Zhu,[62,48] Z. A. Zhu,[1,53] B. S. Zou,[1] and J. H. Zou[1]

(BESIII Collaboration)

[1]*Institute of High Energy Physics, Beijing 100049, People's Republic of China*
[2]*Beihang University, Beijing 100191, People's Republic of China*
[3]*Beijing Institute of Petrochemical Technology, Beijing 102617, People's Republic of China*
[4]*Bochum Ruhr-University, D-44780 Bochum, Germany*
[5]*Carnegie Mellon University, Pittsburgh, Pennsylvania 15213, USA*
[6]*Central China Normal University, Wuhan 430079, People's Republic of China*
[7]*China Center of Advanced Science and Technology, Beijing 100190, People's Republic of China*
[8]*Lahore Campus, COMSATS University Islamabad, Defence Road, Off Raiwind Road, 54000 Lahore, Pakistan*
[9]*Fudan University, Shanghai 200443, People's Republic of China*
[10]*G. I. Budker Institute of Nuclear Physics SB RAS (BINP), Novosibirsk 630090, Russia*
[11]*GSI Helmholtzcentre for Heavy Ion Research GmbH, D-64291 Darmstadt, Germany*
[12]*Guangxi Normal University, Guilin 541004, People's Republic of China*
[13]*Hangzhou Normal University, Hangzhou 310036, People's Republic of China*
[14]*Helmholtz Institute Mainz, Staudinger Weg 18, D-55099 Mainz, Germany*
[15]*Henan Normal University, Xinxiang 453007, People's Republic of China*
[16]*Henan University of Science and Technology, Luoyang 471003, People's Republic of China*
[17]*Huangshan College, Huangshan 245000, People's Republic of China*
[18]*Hunan Normal University, Changsha 410081, People's Republic of China*
[19]*Hunan University, Changsha 410082, People's Republic of China*
[20]*Indian Institute of Technology Madras, Chennai 600036, India*
[21]*Indiana University, Bloomington, Indiana 47405, USA*
[22a]*INFN Laboratori Nazionali di Frascati, INFN Laboratori Nazionali di Frascati, I-00044, Frascati, Italy*
[22b]*INFN Sezione di Perugia, I-06100 Perugia, Italy*
[22c]*University of Perugia, I-06100 Perugia, Italy*
[23a]*INFN Sezione di Ferrara INFN Sezione di Ferrara, I-44122 Ferrara, Italy*
[23b]*University of Ferrara, I-44122 Ferrara, Italy*
[24]*Institute of Modern Physics, Lanzhou 730000, People's Republic of China*
[25]*Institute of Physics and Technology, Peace Avenue 54B, Ulaanbaatar 13330, Mongolia*
[26]*Jilin University, Changchun 130012, People's Republic of China*
[27]*Johannes Gutenberg University of Mainz, Johann-Joachim-Becher-Weg 45, D-55099 Mainz, Germany*
[28]*Joint Institute for Nuclear Research, 141980 Dubna, Moscow Region, Russia*
[29]*Justus-Liebig-Universitaet Giessen, II, Physikalisches Institut, Heinrich-Buff-Ring 16, D-35392 Giessen, Germany*
[30]*Lanzhou University, Lanzhou 730000, People's Republic of China*
[31]*Liaoning Normal University, Dalian 116029, People's Republic of China*
[32]*Liaoning University, Shenyang 110036, People's Republic of China*
[33]*Nanjing Normal University, Nanjing 210023, People's Republic of China*
[34]*Nanjing University, Nanjing 210093, People's Republic of China*
[35]*Nankai University, Tianjin 300071, People's Republic of China*
[36]*North China Electric Power University, Beijing 102206, People's Republic of China*
[37]*Peking University, Beijing 100871, People's Republic of China*
[38]*Qufu Normal University, Qufu 273165, People's Republic of China*
[39]*Shandong Normal University, Jinan 250014, People's Republic of China*
[40]*Shandong University, Jinan 250100, People's Republic of China*

^{41}Shanghai Jiao Tong University, Shanghai 200240, People's Republic of China

^{42}Shanxi Normal University, Linfen 041004, People's Republic of China

^{43}Shanxi University, Taiyuan 030006, People's Republic of China

^{44}Sichuan University, Chengdu 610064, People's Republic of China

^{45}Soochow University, Suzhou 215006, People's Republic of China

^{46}South China Normal University, Guangzhou 510006, People's Republic of China

^{47}Southeast University, Nanjing 211100, People's Republic of China

^{48}State Key Laboratory of Particle Detection and Electronics, Beijing 100049, Hefei 230026, People's Republic of China

^{49}Sun Yat-Sen University, Guangzhou 510275, People's Republic of China

^{50}Suranaree University of Technology, University Avenue 111, Nakhon Ratchasima 30000, Thailand

^{51}Tsinghua University, Beijing 100084, People's Republic of China

^{52a}Turkish Accelerator Center Particle Factory Group, Istanbul Bilgi University, High Energy Physics Research Center,
34060 Eyup, Istanbul, Turkey

^{52b}Near East University, Nicosia, North Cyprus, Mersin 10, Turkey

^{53}University of Chinese Academy of Sciences, Beijing 100049, People's Republic of China

^{54}University of Groningen, NL-9747 AA Groningen, Netherlands

^{55}University of Hawaii, Honolulu, Hawaii 96822, USA

^{56}University of Jinan, Jinan 250022, People's Republic of China

^{57}University of Manchester, Oxford Road, Manchester, M13 9PL, United Kingdom

^{58}University of Minnesota, Minneapolis, Minnesota 55455, USA

^{59}University of Muenster, Wilhelm-Klemm-Strasse 9, 48149 Muenster, Germany

^{60}University of Oxford, Keble Road, Oxford, OX13RH, United Kingdom

^{61}University of Science and Technology Liaoning, Anshan 114051, People's Republic of China

^{62}University of Science and Technology of China, Hefei 230026, People's Republic of China

^{63}University of South China, Hengyang 421001, People's Republic of China

^{64}University of the Punjab, Lahore-54590, Pakistan

^{65a}University of Turin and INFN, University of Turin, I-10125 Turin, Italy

^{65b}University of Eastern Piedmont, I-15121 Alessandria, Italy

^{65c}INFN, I-10125 Turin, Italy

^{66}Uppsala University, Box 516, SE-75120 Uppsala, Sweden

^{67}Wuhan University, Wuhan 430072, People's Republic of China

^{68}Xinyang Normal University, Xinyang 464000, People's Republic of China

^{69}Zhejiang University, Hangzhou 310027, People's Republic of China

^{70}Zhengzhou University, Zhengzhou 450001, People's Republic of China

Based on electron-positron collision data collected with the BESIII detector operating at the Beijing Electron-Positron Collider II storage rings, the value of $R \equiv \sigma(e^+e^- \to \text{hadrons})/\sigma(e^+e^- \to \mu^+\mu^-)$ is measured at 14 center-of-mass energies from 2.2324 to 3.6710 GeV. The resulting uncertainties are less than 3.0% and are dominated by systematic uncertainties.

The lowest-order cross section of $e^+e^- \to$ hadrons, known as the R value in units of the cross section of the QED process $e^+e^- \to \mu^+\mu^-$, is a very important quantity in particle physics [1]. Precision measurements of the R value below 5 GeV contribute to the standard model (SM) prediction of the muon anomalous magnetic moment [2]. The latest direct measurement from Fermilab, when combined with previous measurements, increases the discrepancy between experiment and SM theory to 4.2 standard deviations [3]. The discrepancy is reduced when experiment is compared with recent lattice gauge theory predictions [2,4]. The R value also contributes in the determination of the QED running coupling constant evaluated at the Z pole, i.e., $\alpha(M_Z^2)$. This observable provides another precision test for the SM and is essential for the electroweak precision physics program at future colliders. Many experiments have measured the R value at low energies [5–18], and the latest measurement with the KEDR detector has achieved a precision of better than 3.0% above 3.1 GeV [18].

In this Letter, the R value is measured at 14 center-of-mass (c.m.) energies ($\sqrt{s}$) from 2.2324 to 3.6710 GeV,

where the datasets were collected with the BESIII detector [19] at Beijing Electron-Positron Collider II. The detector has a geometrical acceptance of 93% of the 4π solid angle. It contains a small-celled, helium-based main drift chamber (MDC), a time-of-flight system (TOF) based on plastic scintillators, an electromagnetic calorimeter (EMC) made of CsI(Tl) crystals, a muon system made of resistive plate chambers, and a superconducting solenoid magnet.

Experimentally, the R value is determined with

$$R = \frac{N_{\text{had}}^{\text{obs}} - N_{\text{bkg}}}{\sigma_{\mu\mu}^0 \mathcal{L}_{\text{int}} \varepsilon_{\text{trig}} \varepsilon_{\text{had}} (1 + \delta)}, \qquad (1)$$

where $N_{\text{had}}^{\text{obs}}$ is the number of hadronic events directly counted from data, N_{bkg} is the number of background events remaining after all selection requirements, $\sigma_{\mu\mu}^0 = 4\pi\alpha^2(0)/(3s)$ is the leading-order cross section of $e^+e^- \to \mu^+\mu^-$, $\mathcal{L}_{\text{int}}$ is the integrated luminosity of the data sample, $\varepsilon_{\text{trig}}$ is the trigger efficiency for hadronic events, ε_{had} is the detection efficiency for inclusive hadronic events, and $(1 + \delta)$ is the initial state radiation (ISR) correction factor.

As a first step, $e^+e^- \to e^+e^-$ or $e^+e^- \to \gamma\gamma$ events are identified and then rejected by requiring (i) at least two showers in the EMC, (ii) the angular difference $|\Delta\theta| = |\theta_1 + \theta_2 - 180°|$ less than 10°, where $\theta_{1,2}$ are the polar angles of the two most energetic showers, and (iii) the energy deposition of the second-most energetic shower of the event larger than $0.65E_{\text{beam}}$, where E_{beam} represents the mean energy of the colliding beams.

For the remaining events, good charged hadronic tracks, which are referred to as "prongs" hereafter, are selected by imposing the following requirements: (i) the distance of the closest approach of these tracks to the interaction point (V_z, V_r) is required to be within 5 cm along and 0.5 cm perpendicular to the symmetry axis of the MDC; (ii) the charged tracks must lie in the acceptance region of the MDC, i.e., $|\cos\theta| < 0.93$, where θ is the polar angle of the tracks; (iii) charged tracks that do not originate from the electron-positron collision, such as deuterons, are removed by $\chi_p < 10$ with $\chi_p = (dE/dx - dE/dx_p)/\sigma_p$, where dE/dx is the average energy loss directly measured in the MDC and dE/dx_p is the corresponding value expected for protons with a predicted uncertainty σ_p; (iv) the momenta of these charged tracks should be smaller than $0.94p_{\text{beam}}$, where p_{beam} denotes the mean momentum of the colliding beams; and (v) charged tracks with both $E/(pc) > 0.8$ and $p > 0.65p_{\text{beam}}$ are removed, where E is the deposited energy in the EMC and p is the momentum measured by the MDC. Furthermore, any two oppositely charged tracks both with $E/(pc) > 0.8$ will be regarded as arising from the γ-conversion process [20] and excluded as long as their invariant mass is less than 0.1 GeV/c^2 and their opening angle is less than 15°.

To select hadronic events, at least two good charged tracks are required. For two-prong events, the two charged tracks should not be back-to-back, and the corresponding number of isolated photons ($N_{\text{iso}}^{\text{2-prg}}$) should be larger than 1. Two charged tracks are regarded to be back-to-back as long as both $|\Delta\theta| = |\theta_1 + \theta_2 - 180°| < 10°$ and $|\Delta\phi| = ||\phi_1 - \phi_2| - 180°| < 15°$ are satisfied, where θ and ϕ are the polar and azimuthal angles of the charged tracks, respectively. An isolated photon is selected from showers in the EMC by requiring the deposited energy to be larger than 100 MeV, the opening angle to any charged track to exceed 20°, and the timing of the shower within 700 ns from the start time of the event. For three-prong events, the two charged tracks with highest and second highest momentum must not be back-to-back, and the number of charged tracks with $E/(pc) > 0.8$ should be less than 2. In addition, the number of charged tracks with $r_{\text{PID}} > 0.25$ must be less than 2, where $r_{\text{PID}} = \mathcal{P}(e)/\sum_i \mathcal{P}(i)$, with $i = e, \pi, K, p$ and where $\mathcal{P}(i)$ is the particle identification (PID) probability calculated by combing MDC and TOF information. Events with more than three prongs are directly counted as hadronic events without any additional requirement.

Although the above inclusive hadronic selection criteria are applied, there are still residual background events contributing to $N_{\text{had}}^{\text{obs}}$, coming from lepton pair production, two-photon processes, and beam-associated processes. Simulated data samples produced with a GEANT4-based [21] Monte Carlo (MC) package, which includes the geometric description of the BESIII detector and the detector response, are used to estimate the background yields. The $e^+e^- \to e^+e^-$, $\gamma\gamma$, and $\mu^+\mu^-$ processes are generated by BABAYAGA3.5 [22], while the $e^+e^- \to \tau^+\tau^-$ process is simulated by KKMC [23] with the subsequent decays of τ modeled by EVTGEN [24]. The two-photon processes $e^+e^- \to e^+e^-X$ with $X = e^+e^-, \mu^+\mu^-, \eta, \eta'$, $\pi^+\pi^-$, and K^+K^- [25] are simulated using the generators DIAG36 [26], EKHARA [27] and GALUGA2.0 [28].

Beam-associated background events, which originate from beam-gas interactions and Touschek scatterings, could be misidentified as signal events [19]. An event vertex along the beam direction V_z^{evt}, defined as the average of V_z of all the good charged tracks, and another one $V_{z,\text{loose}}^{\text{evt}}$, taking into account also those tracks not satisfying the V_z requirement, are used to estimate the number of the beam-associated events. In the $|V_{z,\text{loose}}^{\text{evt}}|$ distribution, (0, 5) cm is taken as the signal region and (5, 10) cm as the sideband. All events in the sideband region are assumed to be beam associated. Alternatively, the V_z^{evt} distribution is fitted with a double Gaussian as signal plus a background shape that is obtained from separated-beam data. The two methods give consistent results, which are also confirmed at $\sqrt{s} = 2.4000$ and 3.4000 GeV by directly analyzing the separated-beam data and scaling according to the corresponding data-taking time.

The integrated luminosity is determined by analyzing large-angle Bhabha events at each c.m. energy [29]. The trigger efficiency for hadronic events is nearly 100% [30].

To estimate the hadronic detection efficiency, the LUARLW model, developed to simulate inclusive hadronic events [31,32], is used. After the ISR process, resonance and continuum processes are produced according to the respective cross sections at the effective c.m. energy ($\sqrt{s'}$). All allowed 1^{--} resonances, including $\rho(770)$, $\omega(782)$, $\phi(1020)$, J/ψ, and their excited states are implemented in the LUARLW generator with corresponding resonance parameters taken from the Particle Data Group (PDG) [33]. In the LUARLW generator, the conventional resonances decay according to the branching fractions listed by the PDG, while the hadronic as well as some radiative decays of J/ψ meson and the production of continuum process at any $\sqrt{s'}$ are modeled by the Lund area law [32]. In this area law, a group of parameters controlling the sampling of flavors, multiplicities, and kinematic quantities of generated initial hadrons are tuned according to extensive comparisons between simulation and data in a large number of variables. The agreement after tuning is demonstrated in Fig. 1, where the signal MC sample is compared with data in some of the critical distributions at $\sqrt{s} = 3.4000$ GeV after subtracting the QED-related and beam-associated background contributions. Further comparisons show that the tuned LUARLW MC generator can reasonably reproduce inclusive hadronic events in experimental data at all the c.m. energies utilized in this Letter.

The Feynman diagram (FD) scheme is used to simulate the ISR process in the LUARLW generator and calculate the correction factors $(1 + \delta)$ after formalizing the contribution of the vacuum polarization (VP) correction with the complex expression $1/|1 - \Pi(s)|^2$ instead of the four real terms used in Ref. [10],

$$1 + \delta = \frac{\delta_{\text{vert}}}{|1 - \Pi(s)|^2} + \int_0^{x_m} \frac{F(x, s)}{|1 - \Pi(s')|^2} \frac{\sigma_{\text{had}}^0(s')}{\sigma_{\text{had}}^0(s)} dx. \quad (2)$$

Here, $x = 1 - s'/s$ and $x_m = 1 - 4m_\pi^2/s$ is the maximum allowed energy fraction of the ISR photon in the process $e^+e^- \to \pi^+\pi^-$, δ_{vert} accounts for the contribution of the initial state vertex correction, and $F(x, s)$ denotes the radiator function of the FD scheme [10]. Contributions of leptons and narrow resonances to the VP operator $\Pi(s)$ are calculated analytically [34,35], while that of the remaining hadronic processes is determined via the dispersion relation [10] and the optical theorem [16]. Since $\sigma_{\text{had}}^0(s)$, which parametrizes the lowest-order hadronic cross section from both the continuum and resonance processes, is used as input to $\Pi(s)$ and $(1 + \delta)$, an iterative procedure is performed based on the relation $\sigma_{\text{had}}^0 = R\sigma_{\mu\mu}^0$. The final R value is obtained when the iteration converges.

The systematic uncertainties on the R values are addressed according to the inputs in Eq. (1). All selection criteria are varied around their nominal values to estimate corresponding changes in $N_{\text{had}}^{\text{obs}}$, N_{bkg}, and ε_{had}. The resulting deviations of the R values, which are found to be less than 0.8% for all c.m. energies, are regarded as the systematic uncertainties due to the imperfect reproduction of the data by MC samples. For the uncertainties of the QED-related background estimation, cross checks are performed by using the BABAYAGA NLO [36] package for $e^+e^- \to e^+e^-$ as well as $\gamma\gamma$ processes, and the PHOKHARA [37] generator for $\mu^+\mu^-$ events. For the $e^+e^- \to \tau^+\tau^-$ process, the uncertainty of the KKMC program is negligible, due to the accuracy of the simulation and the small fraction of this background. In addition, the missing two-photon channels like $e^+e^- \to e^+e^-\pi^0$ and the observed contributions from some intermediate states such as the $\rho(770)$ and $f_2(1270)$ in process $e^+e^- \to e^+e^-\pi^+\pi^-$, which are not included in the current two-photon MC samples, are also considered as systematic uncertainties. The total uncertainty of the R values due to QED-related background processes is less than 0.5% due to the small fraction of QED-related events in $N_{\text{had}}^{\text{obs}}$. The difference in the number of the beam-associated background events estimated by the sideband and fit methods, which is found to be less than 0.7%, is taken as the systematic uncertainty. The uncertainty on $\sigma_{\mu\mu}^0$ can be neglected since it can be exactly calculated in QED [34]. The uncertainties of the integrated luminosity and the trigger efficiency are obtained to be 0.8% [29] and 0.1% [30], respectively.

The most crucial sources of systematic uncertainties in this Letter originate from the simulation of the inclusive
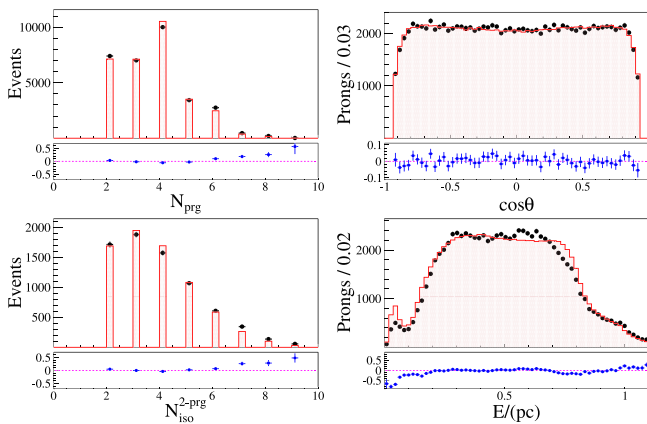

FIG. 1. Comparison between data (black dots) and a simulation based on the LUARLW MC generator (red histograms) at $\sqrt{s} = 3.4000$ GeV. Here, N_{prg} is the number of prongs, and $N_{\text{iso}}^{2\text{-prg}}$ is the number of isolated photons in two-prong events. Track-level variables θ, E, and p stand for the polar angle, deposited energy in EMC, and MDC measured momentum of each prong. The MC simulation distribution is normalized to that in data by the ratio of the corresponding numbers of total events or tracks. The blue dots denote the relative differences.

TABLE I.   Summary of systematic uncertainties (in percent) at each c.m. energy, where the total uncertainty is the sum of the individual ones in quadrature. Uncertainties from the last four sources are correlated between the energy points.

$\sqrt{s}$ (GeV)	Event selection	QED background	Beam background	Luminosity	Trigger efficiency	Signal model	ISR correction	Total
2.2324	0.41	0.23	0.28	0.80	0.10	0.60	1.15	1.62
2.4000	0.55	0.27	0.15	0.80	0.10	1.11	1.10	1.87
2.8000	0.58	0.28	0.34	0.80	0.10	1.97	1.06	2.48
3.0500	0.61	0.33	0.41	0.80	0.10	1.76	1.01	2.33
3.0600	0.60	0.34	0.48	0.80	0.10	1.84	1.00	2.39
3.0800	0.61	0.35	0.35	0.80	0.10	1.31	1.05	2.02
3.4000	0.65	0.33	0.16	0.80	0.10	1.86	1.24	2.49
3.5000	0.60	0.35	0.62	0.80	0.10	2.05	1.16	2.66
3.5424	0.61	0.37	0.01	0.80	0.10	2.05	1.14	2.58
3.5538	0.66	0.31	0.39	0.80	0.10	2.22	1.13	2.74
3.5611	0.74	0.34	0.34	0.80	0.10	2.28	1.12	2.81
3.6002	0.66	0.33	0.38	0.80	0.10	2.27	1.09	2.77
3.6500	0.53	0.35	0.69	0.80	0.10	2.28	1.13	2.83
3.6710	0.61	0.42	0.63	0.80	0.10	2.23	1.04	2.77

hadronic events and the calculation of the ISR correction factors. To estimate the corresponding uncertainties, a composite generator, referred to here as "hybrid," has been developed and investigated intensively [38]. The hybrid generator integrates the CONEXC [39], PHOKHARA, and LUARLW models. CONEXC simulates a total of 47 exclusive processes according to a homogeneous and isotropic phase-space population, but reproducing the measured line shapes of the absolute cross section. PHOKHARA generates ten well-parametrized and established exclusive channels, including $e^+e^- \to \pi^+\pi^-$, $\pi^+\pi^-\pi^0$, $\pi^+\pi^-\pi^0\pi^0$, and $\pi^+\pi^-\pi^+\pi^-$ [37]. The remaining unknown decays of the virtual photon are modeled by LUARLW. To implement as much experimental knowledge as currently available, processes containing intermediate states such as $K^*(892)$, $\omega(782)$, $\phi(1020)$, and η are implemented in the CONEXC component after subtracting their contributions to related inclusive processes to avoid double counting [40]. In addition, a veto procedure has been implemented in the hybrid generator to avoid LUARLW reproducing exclusive processes that are already generated with CONEXC or PHOKHARA. Finally, a set of chosen parameters in the LUARLW component are iteratively tuned and a good consistency between the hybrid simulation and data is achieved. The resulting deviations in $\varepsilon_{\mathrm{had}}$ between the nominal LUARLW generator and the hybrid generator are less than 1.3%. In HYBRID, the structure function scheme [38,41] is used to simulate the ISR process and calculate the corresponding correction factors, where the vacuum polarization operator $\Pi(s)$ is parametrized in Ref. [42]. The maximum difference of the calculated $(1 + \delta)$ factor between the hybrid and LUARLW simulations is 1.4%, which is mainly due to the different parametrization schemes of the ISR process. Since the hadronic detection efficiency is correlated with the ISR correction, the deviations of the resulting R values between these two

simulation schemes, which are less than 2.3% after implementing the same σ_{had}^0 line shape, are regarded as systematic uncertainties. In addition to the different calculation schemes, the accuracy of the FD scheme and the uncertainty of the σ_{had}^0 line shape are considered as uncertainties of the ISR correction factors; the maximum value is less than 1.3% for all the c.m. energies. The systematic uncertainties at each c.m. energy are summarized in Table I.

Table II lists the primary quantities mentioned in Eq. (1) for each energy; the total uncertainty is less than 3.0% and is dominated by systematic effects.

Some additional efforts are made to check the reliability of the R values obtained in this Letter. Dedicated selection criteria are developed to include one-prong events, and the resulting deviation from the nominal R value is at most 0.8%. On the other hand, the exclusion of two-prong events changes the R value by a maximum of 2.2%. To quantitatively verify the LUARLW generator, some exclusive processes are investigated. Production fractions and efficiencies with the nominal inclusive hadronic event selection of the processes $e^+e^- \to \pi^+\pi^-$ and $\pi^+\pi^-\pi^0$ are compared between that of LUARLW and hybrid simulations, respectively. A hypothetical model is constructed by replacing the production fraction and inclusive efficiency of the exclusive process of interest in LUARLW with that of the hybrid generator, which gives a better reproduction of this process due to the inclusion of corresponding experimental knowledge. Differences of resulting $\varepsilon_{\mathrm{had}}$ from the hypothetical and the nominal LUARLW models are less than 2.1% and 0.6% for $\pi^+\pi^-$ and $\pi^+\pi^-\pi^0$ processes, respectively. Similarly, the processes $e^+e^- \to 2(\pi^+\pi^-)$ and $\pi^+\pi^-2\pi^0$ are also studied but with production fractions extracted directly from data. The maximum deviations of $\varepsilon_{\mathrm{had}}$ using these corresponding hypothetical models are found to be 1.1% and 0.6%, respectively. Furthermore, $\varepsilon_{\mathrm{had}}$ changes by 0.2% at $\sqrt{s} = 3.4000$ GeV if the decays of J/ψ

TABLE II.   Summary of primary quantities mentioned in Eq. (1) and the measured R value for each c.m. energy, where the uncertainties are statistical and systematic, respectively.

$\sqrt{s}$ (GeV)	N_{had}^{obs}	N_{bkg}	$\sigma_{\mu\mu}^0$ (nb)	$\mathcal{L}_{int}$ (pb^{-1})	ε_{had} (%)	$1+\delta$	R
2.2324	83 227	2041	17.427	2.645	64.45	1.195	$2.286 \pm 0.008 \pm 0.037$
2.4000	96 627	2331	15.079	3.415	67.29	1.204	$2.260 \pm 0.008 \pm 0.042$
2.8000	83 802	2075	11.078	3.753	72.25	1.219	$2.233 \pm 0.008 \pm 0.055$
3.0500	283 822	7719	9.337	14.89	73.91	1.193	$2.252 \pm 0.004 \pm 0.052$
3.0600	282 467	7683	9.276	15.04	73.88	1.183	$2.255 \pm 0.004 \pm 0.054$
3.0800	552 435	15 433	9.156	31.02	73.98	1.123	$2.277 \pm 0.003 \pm 0.046$
3.4000	32 202	843	7.513	1.733	74.81	1.382	$2.330 \pm 0.014 \pm 0.058$
3.5000	62 670	1691	7.090	3.633	75.32	1.351	$2.327 \pm 0.010 \pm 0.062$
3.5424	145 303	3872	6.921	8.693	75.58	1.341	$2.319 \pm 0.006 \pm 0.060$
3.5538	92 996	2469	6.877	5.562	75.50	1.338	$2.342 \pm 0.008 \pm 0.064$
3.5611	64 650	2477	6.849	3.847	75.50	1.337	$2.338 \pm 0.010 \pm 0.066$
3.6002	159 644	9817	6.701	9.502	75.73	1.328	$2.339 \pm 0.006 \pm 0.065$
3.6500	78 730	6168	6.519	4.760	76.00	1.308	$2.352 \pm 0.009 \pm 0.067$
3.6710	75 253	6461	6.445	4.628	76.11	1.260	$2.405 \pm 0.010 \pm 0.067$

mesons produced in LUARLW are modeled by the hybrid generator, in which a comparably accurate description of the data is observed. The ISR correction factors are also calculated by the structure function scheme mentioned in Ref. [43], and the maximum deviation to the nominally applied FD scheme is 1.3%. The quantity $\varepsilon_{had}(0)(1 + \delta_{obs})$ used in a different R value measurement method in Refs. [11–13] is also calculated, which differs from $\varepsilon_{had}(1 + \delta)$ used in this Letter by 0.8% at most. The deviations observed in these checks are not taken as additional contributions to the systematic uncertainties since they are already covered by the previously discussed systematic uncertainties.

Figure 2 shows the R value obtained in this analysis, together with previous measurements [6,8–18]. A theoretical expectation of R obtained by combining the perturbative QCD prediction [44] and the contributions from involved narrow resonances is also illustrated with
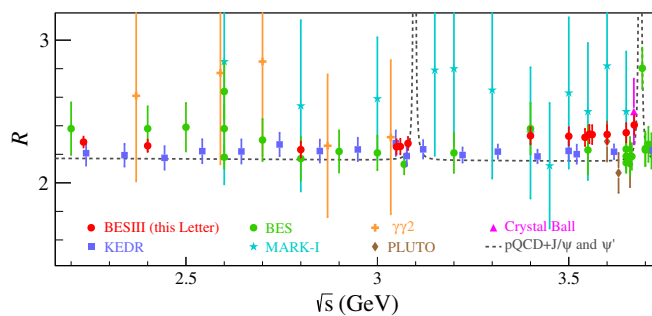

FIG. 2.   Comparison of R values in the c.m. energy region from 2.2 to 3.7 GeV, where the red dots denote that of BESIII, green dots stand for that of BES [11–15], rectangles show KEDR measurements [16–18], orange crosses are R values from the $\gamma\gamma2$ Collaboration [6], cyan stars are that of MARK-I [8], brown diamonds are PLUTO results [9], and the R value of the Crystal Ball Collaboration is shown as a magenta triangle [10].

the dashed curve in Fig. 2. The R values from BESIII have an accuracy of better than 2.6% below 3.1 GeV and 3.0% above. The average R value in the c.m. energy range 3.4–3.6 GeV obtained by BESIII is larger than the corresponding KEDR result and theoretical expectation by 1.9 and 2.7 standard deviations (accounting for 100% correlated systematics from the last four of the seven contributions in Table I), respectively. Further precision measurements are desired and will help to improve the accuracy of the SM predictions of $\alpha(M_Z^2)$, as well as the muon magnetic anomaly, and to verify the QCD sum rules at lower energies [44].

---

[a]Also at the Moscow Institute of Physics and Technology, Moscow 141700, Russia.

[b]Also at Novosibirsk State University, Novosibirsk 630090, Russia.

[c]Also at the NRC "Kurchatov Institute," PNPI, 188300 Gatchina, Russia.

[d]Also at Goethe University Frankfurt, 60323 Frankfurt am Main, Germany.

[e]Also at Key Laboratory for Particle Physics, Astrophysics and Cosmology, Ministry of Education; Shanghai Key Laboratory for Particle Physics and Cosmology; Institute of Nuclear and Particle Physics, Shanghai 200240, People's Republic of China.

[f]Also at Key Laboratory of Nuclear Physics and Ion-Beam Application (MOE) and Institute of Modern Physics, Fudan University, Shanghai 200443, People's Republic of China.

[g]Also at Department of Physics, Harvard University, Cambridge, Massachusetts 02138, USA.

[h]Also at State Key Laboratory of Nuclear Physics and Technology, Peking University, Beijing 100871, People's Republic of China.

[i]Also at School of Physics and Electronics, Hunan University, Changsha 410082, China.

[j]Also at Guangdong Provincial Key Laboratory of Nuclear Science, Institute of Quantum Matter, South China Normal University, Guangzhou 510006, China.

[k]Also at Frontiers Science Center for Rare Isotopes, Lanzhou University, Lanzhou 730000, People's Republic of China.

[l]Also at Lanzhou Center for Theoretical Physics, Lanzhou University, Lanzhou 730000, People's Republic of China.

[m]Present address: Istinye University, 34010 Istanbul, Turkey.

[1] H. M. Hu and X. Y. Li, Int. J. Mod. Phys. A, **24**, 111 (2009).

[2] T. Aoyama, N. Asmussen, M. Benayoun *et al.*, Phys. Rep. **887**, 1 (2020).

[3] B. Abi *et al.* (Muon $g - 2$ Collaboration), Phys. Rev. Lett. **126**, 141801 (2021).

[4] Sz. Borsanyi *et al.*, Nature (London) **593**, 51 (2021).

[5] P. A. Rapidis, B. Gobbi, D. Luke, A. Barbaro-Galtieri, J. M. Dorfan *et al.*, Phys. Rev. Lett. **39**, 526 (1977).

[6] C. Bacci *et al.* ($\gamma\gamma2$ Collaboration), Phys. Lett. **86B**, 234 (1979).

[7] R. H. Schindler *et al.*, Phys. Rev. D **21**, 2716 (1980).

[8] J. L. Siegrist, R. F. Schwitters, M. S. Alam, A. M. Boyarski, M. Breidenbach *et al.*, Phys. Rev. D **26**, 969 (1982).

[9] L. Criegee, and G. Knies (PLUTO Collaboration), Phys. Rep. **83**, 151 (1982).

[10] A. Osterheld *et al.*, SLAC Report No. SLAC-PUB-4160, 1986.

[11] J. Z. Bai *et al.* (BES Collaboration), Phys. Rev. Lett. **84**, 594 (2000).

[12] J. Z. Bai *et al.* (BES Collaboration), Phys. Rev. Lett. **88**, 101802 (2002).

[13] M. Ablikim *et al.* (BES Collaboration), Phys. Lett. B **677**, 239 (2009).

[14] M. Ablikim *et al.* (BES Collaboration), Phys. Lett. B **641**, 145 (2006).

[15] M. Ablikim *et al.* (BES Collaboration), Phys. Rev. Lett. **97**, 262001 (2006).

[16] V. V. Anashin *et al.* (KEDR Collaboration), Phys. Lett. B **753**, 533 (2016).

[17] V. V. Anashin *et al.* (KEDR Collaboration), Phys. Lett. B **770**, 174 (2017).

[18] V. V. Anashin *et al.* (KEDR Collaboration), Phys. Lett. B **788**, 42 (2019).

[19] M. Ablikim *et al.* (BESIII Collaboration), Nucl. Instrum. Methods Phys. Res., Sect. A **614**, 345 (2010).

[20] Z. R. Xu and K. L. He, Chin. Phys. C **36**, 742 (2012).

[21] S. Agostinelli *et al.* (GEANT4 Collaboration), Nucl. Instrum. Methods Phys. Res., Sect. A **506**, 250 (2003).

[22] C. M. Carloni Calame, C. Lunardini, G. Montagna, O. Nicrosini, and F. Piccinini, Nucl. Phys. **B584**, 459 (2000); Nucl. Phys. B, Proc. Suppl. **131**, 48 (2004).

[23] S. Jadach, B. F. L. Ward, and Z. Wąs, Comput. Phys. Commun. **130**, 260 (2000); Phys. Rev. D **63**, 113009 (2001).

[24] D. J. Lange, Nucl. Instrum. Methods Phys. Res., Sect. A **462**, 152 (2001); R. G. Ping, Chin. Phys. C **32**, 599 (2008).

[25] V. M. Budnev, I. F. Ginzburg, G. V. Meledin, and V. G. Serbo, Phys. Rep. **15**, 181 (1975).

[26] F. A. Berends, P. H. Daverveldt, and R. Kleiss, Comput. Phys. Commun. **40**, 285 (1986).

[27] H. Czyz, P. Kisza, and S. Tracz, Phys. Rev. D **97**, 016006 (2018).

[28] G. A. Schuler, Comput. Phys. Commun. **108**, 279 (1998).

[29] M. Ablikim *et al.* (BESIII Collaboration), Chin. Phys. C **41**, 063001 (2017).

[30] K. Zhu, Z.-A. Liu, D.-P. Jin, H. Xu, W.-X. Gong, K. Wang, and G.-F. Cao, Chin. Phys. C **34**, 1779 (2010).

[31] B. Andersson, *The Lund Model* (Cambridge University Press, Cambridge, England, 1998).

[32] B. Andersson and H. M. Hu, arXiv:hep-ph/9910285.

[33] P. A. Zyla *et al.* (Particle Data Group), Prog. Theor. Exp. Phys. **2020**, 083C01 (2020).

[34] W. Greiner and J. Reinhardt, *Quantum Electrodynamics* (Springer, New York, 2002), p. 292.

[35] A. G. Shamov *et al.* (KEDR Collaboration), Chin. Phys. C **34**, 836 (2010).

[36] G. Balossini, C. M. Carloni Calame, G. Montagna, O. Nicrosini, and F. Piccinini, Nucl. Phys. **B758**, 227 (2006); Phys. Lett. B **663**, 209 (2008).

[37] G. Rodrigo, H. Czyz, J. H. Kuhn, and M. Szopa, Eur. Phys. J. C **24**, 71 (2002); H. Czyz, J. H. Kuhn, and A. Wapienik, Phys. Rev. D **77**, 114005 (2008); H. Czyz and J. H. Kuhn, Phys. Rev. D **80**, 034035 (2009).

[38] R. G. Ping, X.-A. Xiong, L. Xia, Z. Gao, Y.-T. Li, X.-Y. Zhou, B.-X. Zhang, B. Zheng, W.-B. Yan, H.-M. Hu, and G.-S. Huang, Chin. Phys. C **40**, 113002 (2016).

[39] R. G. Ping *et al.*, Chin. Phys. C **38**, 083001 (2014).

[40] For example, and the process $e^+e^- \to K^{*0}K^-\pi^+$, which is fully simulated in the CONEXC component of the hybrid generator, can also contribute to the implemented inclusive process $e^+e^- \to K^+K^-\pi^+\pi^-$ due to the decay $K^{*0} \to K^+\pi^-$. Therefore, this contribution should be subtracted from the inclusive process in advance.

[41] O. Nicrosini and L. Trentadue, Nucl. Phys. **B318**, 1 (1989).

[42] F. Jegerlehner, Z. Phys. C **32**, 195 (1986).

[43] E. A. Kureav and V. S. Fadin, Sov. J. Nucl. Phys. **41**, 466 (1985).

[44] P. A. Baikov, K. G. Chetyrkin, J. H. Kühn, and J. Rittinger, Phys. Lett. B **714**, 62 (2012).